MISCELLANEOUS FIELD STUDIES MAP MF-2268 SHEET 1 OF 2

GLORIA sidescan-sonar data. A 160-in³ airgun was fired at 10-s intervals,

and data were recorded digitally at sea using a two-channel hydrophone

streamer. Sidescan-sonar mosaics and unprocessed seismic-reflection,

bathymetric, and magnetic profiles collected on these cruises are presented in

EEZ-Scan 87 Scientific Staff (1991). Additional seismic-reflection lines were

run on the RV Cape Hatteras in 1991. These lines were collected using a

120-in³ airgun fired at 10-s intervals and also recorded digitally at sea from a

two-channel hydrophone streamer. The tracks for all of these two-channel

thickness of the gas-hydrate-stable zone were made, are shown in figures 4,

the BSR are present, the following processes and process parameters were

used: debias, mute, gain proportional to first power of traveltime,

deconvolution (design window = 0-1.4 s below the sea floor; filter length =

0.16 s; prewhitening = 10 percent; prediction distance = 0.02 s), bandpass

filter (passed between 10 and 100 Hz), and two-channel stack. The stack

summed the two channels with no moveout correction applied, and served to

increase the signal-to-noise ratio compared to single-channel display. This

processing strategy preserved relative true amplitude. From these processed

data, median reflectance was estimated for a window extending from 250 to

500 ms below the sea floor (within the gas-hydrate-stable zone), and a plot

was created of median reflectance along the profile with a moving median

Median reflectance plots along each two-channel seismic-reflection profile

(tracks shown in figures 4, 5, and 6) allowed assignment of average hydrate-

(fig. 7B). Using this calibration as a guide, an interpretation of the areal

extent of each class was drawn on each seismic section; an example of this

technique is shown in figure 7A. Then each of these interpretations was

digitized and the values of thickness in acoustic traveltime of each blanking

class were multiplied by appropriate velocities for that class (table 1) at

intervals along the tracklines. A summary of the volume distribution of

deposits representing each class was made by integrating between the

calculation points using a surface-modeling, gridding, and contouring program

(Interactive Surface Modeling [ISM], developed by Dynamic Graphics, Inc.).

average proportion of gas hydrate for that class, and the results for the three

classes were summed. This resulted in the estimate of total volume of gas

hydrate within the study area that is shown by the isopach contours in figure

4. The quantity of hydrate is expressed by contours showing inferred total

volume of hydrate existing within the sediments; that is, the amount of hydrate

that would appear if all the hydrate that is dispersed in the sediments from the

sea floor to the BSR were extracted and piled on the sea floor above. In areas

where hydrate is most concentrated, total thickness is greater than 45 m,

although this is distributed throughout the few hundred meters of sediment

above the BSR. The hydrate is likely to be disseminated in the sediment as

small grains and also to be concentrated in nodules, veins, and layers. To

show where hydrate is most concentrated we also present a similar map

showing the distribution of hydrate that exists in Class I deposits (fig. 5).

Most concentrations of gas hydrate represent locations where sedimentation

rates either are high presently or have been high in the geologically recent

past, because these are areas where organic material is preserved and

converted to biogenic gas by bacteria in the sediments (Dillon and others,

calculate the volume of hydrate in specific areas and the amount of gas that

would be required to form this much hydrate. The volume of natural gas in

gas hydrate at standard temperature and pressure is about 160 times the

volume of the hydrate as a crystalline solid. Two areas of high hydrate

concentration were selected to make these estimates, indicated by diagonal

hatching in figure 4. The first, represented by the large rectilinear polygon

is located between approximately lat 31.2° to 33.8° N. and long 74.8° to

76.5° W. The second area, which is within the larger rectilinear area, is

is defined by the 30-m contour of total hydrate and located between

irregularly shaped. It is a region of unusually high hydrate concentration that

approximately lat 31.4° to 32.1° N. and long 74.9° to 76.1° W. Table 2

presents the estimates of hydrate and gas in the two areas. Areas are given

in square kilometers, volumes in cubic meters and in trillion cubic feet (TCF),

Table 2.--Estimated hydrate and gas volumes and carbon mass in selected

Large polygon 20,200 4.87×10^{11} 7.8×10^{13} 2750 42.330-m contour 3,050 1.12×10^{11} 1.8×10^{13} 630 9.7

For purposes of comparison, the consumption of gas in the United States in

at any given point was calculated by identifying the thickness in acoustic traveltime for deposits of each class and multiplying the time-thickness of each

class by a characteristic velocity associated with that class (table 1). These

thicknesses were then summed to get the total depth to the base of the gas

hydrate. Velocities used were as follows: Class I, 2 km/s; Class II, 1.9

km/s; and Class III, 1.8 km/s. Because gas hydrate is stable to higher

temperatures as pressure increases and because pressure increases as water

deepens, the base of hydrate stability might be expected to extend deeper into

depends only on change of water depth and that the thermal and chemical regimes are constant. This simple seaward thickening of the gas-hydratestable zone does not occur, however. Clearly, the structure of the gas-hydrate zone is far more complicated than anticipated and thus is affected by factors

the sediments as water depth increases. This assumes that pressure change

Figure 6 is a map of the depth of the BSR below the sea floor. The interval from the sea floor down to the BSR represents the zone in which gas hydrate is stable. This map, like figures 4 and 5, was created using th seismic data and the interpretation of blanking classes. The depth of the BSR

Hydrate Methane Methane Carbon

areas, indicated by diagonal hatching in figure 4

and mass of carbon in gigatons (Gt).

Having mapped the estimated volume of gas hydrate, it is possible to

To map total hydrate, the volume of each class was multiplied by the

blanking-class level (I, II, or III) within the selected 250- to 500-ms window

applied (fig. 7B).

1993, 1994).

seismic-reflection profiles, from which estimates of amount of gas hydrate and

To enhance the appearance of the subbottom region where blanking and

Initially, interval velocity and median reflectance were determined for a layer 250 milliseconds (ms) thick within the gas-hydrate-cemented zone (above

hydrate-cemented sediment replaces non-hydrate-bearing sediment in

< 0.024

0.05 - 0.0251.94–2.02 1.85–1.94 1.7–1.85

Data Collection and Processing

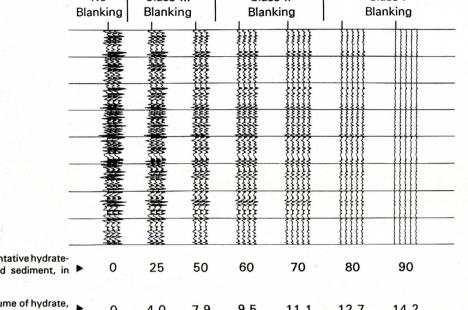
The majority of the seismic-reflection lines used in this study were collected during five cruises of the research vessel (RV) Farnella conducted between February and May 1987, which were intended primarily to gather

cemented sediment, in ▶ 0 25 50 60 70 80 90

of digital seismic data that is available in a grid dense enough to allow mapping is vertical-incidence seismic data. Vertical-incidence data is collected with no offset (horizontal separation between seismic source and receiver), and therefore it does not allow the calculation of interval velocities but does allow the measurement of blanking. Our strategy to estimate hydrate concentration in the study area consisted of the following steps: (1) quantify interval velocity and amplitude blanking in the hydrate-cemented zone in the few available multichannel seismic-reflection profiles in the study area; (2) estimate the amount of hydrate indicated by velocity; (3) establish the relation between hydrate and blanking; and (4) apply this relation to measure hydrate concentrations indicated by blanking in the vertical-incidence data (Lee and

the BSR) in six U.S. Geological Survey multichannel seismic profiles located in the survey area (not shown on maps, as they were not used for the final hydrate analysis). Blanking is measured as the decrease in median reflectance within the layer. Median reflectance is the seismic amplitude adjusted for factors other than hydrate cementation that are also known to affect amplitude; these are travel distance due to water depth variations, and sea-floor reflectivity. Concentrations of gas hydrate were calculated using the known velocities of rock (the sediment grains), water, and hydrate, and the porosity, which is the proportion of sediment volume occupied by water plus hydrate. The porosity of near-bottom sediments off the southeastern United States was estimated from results of scientific drilling (Hollister, Ewing and others, 1972; Sheridan, Gradstein and others, 1983). Once the hydrate concentrations for the six multichannel seismic lines were calculated, variations in concentration of hydrate could be correlated with the measured blanking. This relation then was used to estimate the proportion of hydrate in the vertical-incidence, two-channel profiles for which the calculation of velocity was not possible. The relation of blanking to hydrate concentration is not considered to be precise, so in estimating blanking in seismic profiles we divided the effect into only three blanking classes. Class boundaries were selected at amplitude reductions of 6 decibels. To illustrate how the presence of increased amounts of gas hydrate cement in sediments affects seismic reflections, and to show the three classes of blanking, we modeled a series of synthetic seismograms (fig. 3). In order to simulate a seismogram for non-cemented sediments, 200 random porosities in the porosity range of 50–70 percent (similar to the range in measurements for the study area) were generated and the corresponding velocities and densities were computed. We then computationally "replaced" non-hydrate-cemented sediment with increasing amounts of a representative hydrate-cemented sediment (hydrate concentration 27.5 percent, porosity 57.5 percent); velocities and densities were modified accordingly. A reflection coefficient series was computed on the basis of the modified velocities and densities and an appropriate bandpass filter was applied. In illustrating the effect on blanking of increasing proportions of gas-hydrate cement, figure 3 shows a series of synthetic seismograms, in which the representative

Table 1.--Properties of the blanking classes of gas-hydrate-cemented



Bulk volume of hydrate, ▶ 0 4.0 7.9 9.5 11.1 12.7 14.2 Figure 3.--Synthetic seismograms showing the calculated effect (from left to right) of the increase of hydrate content on reflection amplitudes. The reduction in amplitude, which apparently is caused by cementation of reflecting layers by gas hydrate, is known as "blanking". Blanking class boundaries are indicated. Class I

> Conclusions These maps represent the first effort to estimate the volume of gas hydrate and structure of the gas-hydrate zone over a significant region. Thus they are an important early step in analyzing the significance of gas hydrate as a possible energy resource, as a control on sea-floor stability, and as a possible reservoir of a greenhouse gas, methane.

other than pressure alone (Dillon and others, 1993, 1994).

Acknowledgments We wish to thank Rodney Malone of the Morgantown Energy Technology Center, U.S. Department of Energy, for his support and continued interest in studies of gas hydrate in the natural environment. Reviews by James M. Robb and Lawrence J. Poppe, U.S. Geological Survey, were extremely valuable.

References Cited Brandt, H., 1960, Factors affecting compressional wave velocity in unconsolidated marine sand sediments: Journal of the Acoustical Society of America, v. 32, p. 171–179. Collins, B.P., and Watkins, J.S., 1985, Analysis of a gas hydrate off southwest Mexico using seismic processing techniques and Deep Sea Drilling Project Leg 66 results: Geophysics, v. 50, no. 1, p. 16-24.

Dillon, W.P., Grow, J.A., and Paull, C.K., 1980, Unconventional gas-hydrate seals may trap gas off southeast U.S.: Oil and Gas Journal, v. 78, no. 1, p. 124–130. Dillon, W.P., Lee, M.W., and Coleman, D.F., 1994, Identification of marine hydrates in situ and their distribution off the Atlantic coast of the United States: International Conference on Natural Gas Hydrates: Annals of the New York Academy of Sciences, v. 715, p. 364-380. Dillon, W.P., Lee, M.W., Fehlhaber, Kristen, and Coleman, D.F., 1993, Gas hydrates on the Atlantic continental margin of the United States--controls

on concentration, in Howell, D.G., ed., The future of energy gases: U.S. Geological Survey, Professional Paper 1570, p. 313–330. Dillon, W.P., and Paull, C.K., 1983, Marine gas hydrates--II: Geophysical evidence, in Cox, J. L., ed., Natural gas hydrates--properties, occurrences and recovery: Boston, Mass., Butterworth Publishers, p. 73–90. EEZ-Scan 87 Scientific Staff, 1991, Atlas of the U.S. Exclusive Economic Zone, Atlantic continental margin: U.S. Geological Survey, Miscellaneous Investigations Series I–2054, 174 p. Hollister, C.D., Ewing, J.I., and others, 1972, Initial reports of the Deep Sea Drilling Project, v. 11: Washington, D.C., U.S. Government Printing

Krason, J., and Ridley, W.I., 1985, Geological evolution and analysis of confirmed or suspected gas hydrate localities: v. 1, Blake-Bahama Outer Ridge--U.S. East Coast: U.S. Department of Energy, Technical Information Center, report no. DOE/MC/21181 (DE86001006), 100 p. Kvenvolden, K.A., 1988, Methane hydrate--a major reservoir of carbon in the shallow geosphere?, in Schoell, Martin, ed., Origins of methane in the Earth: Chemical Geology, v. 71, no. 1-3, p. 41-51. Kvenvolden, K.A., and Barnard, L.A., 1982, Hydrates of natural gas in continental margins, in Watkins, J.S., and Drake, C.L., eds., Studies in continental margin geology: American Association of Petroleum Geologists, Memoir No. 34, p. 631–640. 1983, Gas hydrates of the Blake Outer Ridge, Site 533, Deep Sea

Drilling Project Leg 76, in Sheridan, R.E., Gradstein, F.M., and others, Initial reports of the Deep Sea Drilling Project, v. 76: Washington, D.C. U.S. Government Printing Office, p. 353-365. Kvenvolden, K.A., and Kastner, Miriam, 1990, Gas hydrates of the Peruvian outer continental margin, in Suess, Erwin, von Huene, Roland, and others, Proceedings of the Ocean Drilling Program, scientific results, v. 112: College Station, Tex., Ocean Drilling Program, Texas A&M University, p. 517–526. Lee, M.W., Dillon, W.P., and Hutchinson, D.R., 1992, Estimating the

amount of gas hydrate in marine sediments in the Blake Ridge area, southeastern Atlantic margin: U.S. Geological Survey, Open-File Report Lee, M.W., Hutchinson, D.R., Agena, W.F., Dillon, W.P., Miller, J.J., and Swift, B.A., 1994, Seismic character of gas hydrates on the southeastern U.S. continental margin: Marine Geophysical Researches, v. 16, p.

Swift, B.A., 1993a, Method of estimating the amount of in-situ gas hydrates in deep marine sediments: Marine and Petroleum Geology, v. 10, no. 5, p. 493–506. 1993b, Use of seismic data in estimating the amount of in-situ gas hydrates in deep marine sediment, in Howell, D.G., ed., The future of energy gases, U.S. Geological Survey, Professional Paper 1570, p.

Lee, M.W., Hutchinson, D.R., Dillon, W.P., Miller, J.J., Agena, W.F., and

Miller, J.J., Lee, M.W., and von Huene, Roland, 1991, An analysis of a seismic reflection from the base of a gas hydrate zone, offshore Peru: American Association of Petroleum Geologists Bulletin, v. 75, no. 5, p. Paull, C.K., and Dillon, W.P., 1981, Appearance and distribution of the gas

hydrate reflection in the Blake Ridge region, offshore southeastern United States: U.S. Geological Survey, Miscellaneous Field Studies Map

Rowe, M.M., and Gettrust, J.F., 1993, Fine structure of methane bearing sediments on the Blake Outer Ridge as determined from deep-tow multichannel seismic data: Journal of Geophysical Research, v. 98, p. Sheridan, R.E., Gradstein, F.M., and others, 1983, Initial reports of the Deep Sea Drilling Project, v. 76: Washington, D.C., U.S. Government Printing Office, 947 p.

Shipley, T.H., and Didyk, B.M., 1982, Occurrence of methane hydrates offshore southern Mexico, in Watkins, J.S., Moore, J.C., and others, Initial reports of the Deep Sea Drilling Project, v. 66: Washington, D.C., U.S. Government Printing Office, p. 547-555. Shipley, T.H., Houston, M.H., Buffler, R.T., Shaub, F.J., McMillen, K.J.,

Ladd, J.W., and Worzel, J.L, 1979, Seismic evidence for widespread possible gas hydrate horizons on continental slopes and rises: American Association of Petroleum Geologists Bulletin, v. 63, no. 12, p. Sloan, E.D., Jr., 1990, Clathrate hydrates of natural gases: New York, Marcel Dekker, Inc., 641 p.

Tucholke, B.E., Bryan, G.M., and Ewing, J.I., 1977, Gas-hydrate horizons detected in seismic-profiler data from the western North Atlantic: American Association of Petroleum Geologists Bulletin, v. 61, no. 5, p.

> **AUTHOR AFFILIATIONS** ¹Woods Hole, MA 02543 ²Denver, CO 80225–0045

Manuscript approved for publication April 4, 1994 Any use of trade, product, or firm names in this publication is for descriptive purposes only and does not imply endorsement by the U.S. Government For sale by U.S. Geological Survey, Information Services, Box 25286, Federal Center, Denver, CO 80225